

Published in final edited form as:

Nat Nanotechnol. ; 6(8): 524–531. doi:10.1038/nnano.2011.101.

Cell-surface sensors for real-time probing of cellular environments

Weian Zhao^{1,2,3,4}, **Sebastian Schafer**^{1,2,3,4}, **Jonghoon Choi**⁵, **Yvonne J. Yamanaka**^{5,6}, **Maria L. Lombardi**⁷, **Suman Bose**⁸, **Alicia L. Carlson**^{2,9}, **Joseph A. Phillips**^{1,2,3,4}, **Weisuong Teo**^{1,2,3,4}, **Iliia A. Droujinine**^{1,2,3,4}, **Cheryl H. Cui**^{1,2,3,4}, **Rakesh K. Jain**¹⁰, **Jan Lammerding**⁷, **J. Christopher Love**⁵, **Charles P. Lin**^{2,3,9}, **Debanjan Sarkar**^{1,2,3,4}, **Rohit Karnik**⁸, and **Jeffrey M. Karp**^{1,2,3,4,*}

¹Center for Regenerative Therapeutics & Department of Medicine, Brigham & Women's Hospital, 65 Landsdowne Street, Cambridge, Massachusetts 02139, USA

²Harvard Medical School, 65 Landsdowne Street, Cambridge, Massachusetts 02139, USA

³Harvard Stem Cell Institute, 65 Landsdowne Street, Cambridge, Massachusetts 02139, USA

⁴Harvard-MIT Division of Health Science and Technology, 65 Landsdowne Street, Cambridge, Massachusetts 02139, USA

⁵Department of Chemical Engineering, Massachusetts Institute of Technology, 77 Massachusetts Avenue, Cambridge, Massachusetts 02139, USA

⁶Department of Biological Engineering, Massachusetts Institute of Technology, 77 Massachusetts Avenue, Cambridge, Massachusetts 02139, USA

⁷Department of Medicine, Brigham and Women's Hospital/Harvard Medical School, 65 Landsdowne Street, Cambridge, Massachusetts 02139, USA

⁸Department of Mechanical Engineering, Massachusetts Institute of Technology, 77 Massachusetts Avenue, Cambridge, Massachusetts 02139, USA

⁹Wellman Center for Photomedicine and Center for Systems Biology, Massachusetts General Hospital/Harvard Medical School, 40 Blossom Street, Boston, Massachusetts 02114, USA

¹⁰Edwin L. Steele Laboratory, Department of Radiation Oncology, Massachusetts General Hospital/Harvard Medical School, 55 Fruit Street, Boston, Massachusetts 02114, USA.

Abstract

The ability to explore cell signalling and cell-to-cell communication is essential for understanding cell biology and developing effective therapeutics. However, it is not yet possible to monitor the interaction of cells with their environments in real time. Here, we show that a fluorescent sensor attached to a cell membrane can detect signalling molecules in the cellular environment. The

© 2011 Macmillan Publishers Limited. All rights reserved.

* jkarp@rics.bwh.harvard.edu .

Author contributions

W.Z. and J.M.K. are responsible for study concept and design. W.Z., J.M.K., J.L., J.C.L., C.P.L., D.S. and R.K. prepared the manuscript. W.Z., S.S., J.C., Y.J.Y., M.L.L., S.B., A.L.C., J.A.P, W.T., I.A.D. and C.C. carried out experiments and performed data analysis. R.K.J. provided genetically engineered cells.

Animals and intravital confocal microscopy. See Supplementary Information.

Additional information

The authors declare no competing financial interests. Supplementary information accompanies this paper at

www.nature.com/naturenanotechnology. Reprints and permission information is available online at <http://www.nature.com/reprints/>.

Correspondence and requests for materials should be addressed to J.M.K.

sensor is an aptamer (a short length of single-stranded DNA) that binds to platelet-derived growth factor (PDGF) and contains a pair of fluorescent dyes. When bound to PDGF, the aptamer changes conformation and the dyes come closer to each other, producing a signal. The sensor, which is covalently attached to the membranes of mesenchymal stem cells, can quantitatively detect with high spatial and temporal resolution PDGF that is added in cell culture medium or secreted by neighbouring cells. The engineered stem cells retain their ability to find their way to the bone marrow and can be monitored *in vivo* at the single-cell level using intravital microscopy.

Monitoring cell functions and cell-to-cell communication in the cellular environment has enormous implications for cell biology and regenerative medicine¹. In the area of cell therapy there is also significant interest in better understanding and tracking the fate of transplanted cells^{2,3}. Unfortunately, probing what cells 'see' and how they respond in real time to surrounding signals (i.e. cytokines) is still a major challenge¹. Conventional assays, including flow cytometry, enzyme-linked immunosorbent assay (ELISA), immunostaining and polymerase chain reaction are valuable, but typically require stepwise staining, washing or manipulation before analysis. Alternative approaches include staining cells with metabolically and chemically engineered probes or nanoparticles⁴⁻⁶. However, most of these assays measure markers under 'static' conditions and fail to monitor what cells sense in real time, in a dynamic manner.

Fluorescence resonance energy transfer (FRET) sensors, particularly those using genetically engineered proteins, have offered a way to study protein expression, migration, conformational change and protein-protein interactions, as well as to probe metal ions and enzyme activities inside cells or on cell surfaces⁶⁻¹⁰. In addition, B cells have been engineered as sensors for the identification of pathogens; for example, a calcium-sensitive bioluminescent protein engineered onto cells emits light in the presence of pathogens¹¹. Others have reported a luciferase-engineered cell approach that detects the local concentration of ATP at the cell surface¹². However, these approaches require complex genetic engineering methods and cannot probe multiple markers simultaneously. Recently, the cell membrane has been engineered using chromatic polymer patches that produce light in the presence of cell-membrane-disrupting molecules¹³. Although useful for predicting the cytotoxicity of molecules that perturb the cell membrane, this approach lacks potential for the general study of cell signalling.

In this Article, we present a simple, generic approach to using real-time probes at the cell surface for examining intercellular signalling within the cellular environment using nucleic acid aptamer sensors (Scheme 1). Specifically, we covalently attached fluorescent aptamer sensors to the surface of cells to produce a real-time signal when target molecule(s) contact the cell surface. Aptamers are single-stranded oligonucleotides that can be generated for a target molecule by an *in vitro* selection process (systematic evolution of ligands by exponential enrichment; SELEX) with high affinity¹⁴⁻¹⁹. Aptamers can be readily engineered for therapeutics or as probes for targeting, imaging or biosensing by introducing functional moieties including modified nucleotides, biotin or dyes during the chemical synthesis¹⁶⁻²².

We have focused on attaching an aptamer that recognizes the platelet-derived growth factor (PDGF) onto the membrane of mesenchymal stem cells (MSCs). The use of MSCs is attractive because they can differentiate into different types of cells, including osteoblasts, adipocytes and chondroblasts, and they can promote angiogenesis and have immunomodulatory effects². MSCs are currently being tested in over 100 clinical trials to regenerate damaged tissue and treat inflammation^{2,23}. Although the clinical trials have met safety endpoints, some have recently failed to show efficacy²³ and this is attributed in part to an incomplete understanding of MSC biology, particularly how MSCs signal in their niche

environment and communicate with other cells (i.e. endothelial cells, immune cells and cancer cells)^{2,23}. We address this issue by constructing sensors for detecting PDGF, a potent chemoattractant that recruits MSCs to inflamed tissue and tumours, and an important signalling molecule in the participation of MSCs in vascular regeneration and communication with activated endothelial cells or tumour cells^{24–26}. Importantly, PDGF aptamers and simple aptamer-based PDGF sensors have been described^{27–29}.

We envision that cell surface sensors can be delivered into a particular *in vivo* niche by means of delivery of an exogenous cell source. In particular, MSCs have been shown to home to sites of inflammation, bone marrow and to tumours². Imaging of transplanted cells can then be achieved by intravital confocal microscopy (IVM), which has been used previously in the study of stem cell and leukocyte trafficking, cell functions and cell–cell interactions *in vivo*^{1,30–32}. Through the combination of cell-surface sensors, cell homing and IVM, we hope the cell sensors can be used to study intercellular signalling and cellular microenvironments in real time, at single-cell resolution, in living animals.

Engineering aptamer sensors on the cell surface

A PDGF sensor based on a previously isolated aptamer sequence has already been engineered^{27–29}. This PDGF sensor harnesses aptamer conformational changes that occur when binding to PDGF, which brings two attached dyes within close proximity; the crosstalk between the two dyes yields a fluorescence signal (Fig. 1a). This sensor is highly selective and detects PDGF in the picomolar range by producing an instantaneous signal^{27,28}. However, these sensors were designed to operate in the solution phase and contain dyes at each end of the aptamer (Fig. 1a,b)^{27,28}. To enable binding to the cell surface, we first engineered the aptamer sensor to have a surface anchoring moiety. As shown in Fig. 1c,d, the original single-stranded PDGF aptamer is extended at one end by a short oligonucleotide that can hybridize with its complementary strand (details of DNA sequences are provided in Supplementary Table S1). Two dyes, at desirable positions, and anchor moieties (i.e. biotin) can be accommodated easily on these two separated strands during DNA synthesis, and can then be annealed together before anchoring onto cells.

The original PDGF sensor developed by Tan's group undergoes non-specific folding that occurs in the presence of divalent metal ions (i.e. Mg^{2+} and Ca^{2+}) and thus produces a high background, making it unsuitable for physiological conditions (Fig. 1b)^{27,28}. To overcome this issue, we mutated the aptamer sequence by changing a C–G base pair in the stem to an A–G non-base pair. Such a mutation and the above-mentioned two-stranded sensor design did not significantly impair the aptamer binding ability. We engineered two types of sensors: a quench sensor (FAM/Dabcyl) (Fig. 1c) and a FRET sensor (Cy3/Cy5) (Fig. 1d). The sensors showed robust performance in the presence of divalent metal ions (phosphate buffered saline, PBS +/+) (Supplementary Fig. S1). Note also that a temperature change (in the range from room temperature to 37 °C) does not have a significant impact on the binding affinity of the aptamer to PDGF; rather, an elevated temperature (i.e. 37 °C) disrupts the duplex stem and drives the equilibrium to the unfolded state in the absence of PDGF, which therefore produces a higher (beneficial) signal-to-noise ratio (Fig. 1b and data not shown).

The simple chemistry approach of attaching sensors on the cell membrane bypasses the complex genetic, enzymatic or metabolic engineering approaches used previously for modifying the cell surface. Specifically, our cell modification procedure consists of three steps involving treating cell surface amines with sulphonated biotiny-*N*-hydroxy-succinimide (NHS–biotin), followed by streptavidin–biotin interactions (Fig. 2)^{33,34}. Previously, using dye-conjugated molecules and flow cytometry, we showed that the cell surface coverage (of biotin, streptavidin or target ligand) at each step can be controlled by

adjusting the reagent concentration and reaction times during conjugation³⁵ (D. Sarkar *et al.*, data not shown). Approximately 21,000 molecules are typically attached on each MSC (D. Sarkar *et al.*, data not shown). This method for functionalizing the surface and the presence of ligands on the cell surface did not affect the cell phenotype or homing ability^{33–35} (D. Sarkar *et al.*, unpublished observations).

The quench sensor (Fig. 1c) functioned well on the cell surface, and the addition of PDGF resulted in a decrease in fluorescence (Fig. 3). Sensors on the cell surface respond to PDGF within seconds; the sensor signal quantitatively correlates with the concentration of PDGF added into the cell solution (Fig. 3b) and is specific to PDGF (Supplementary Fig. S2). Because the quench sensor does not have an internal reference and the signal may be influenced by external factors (including sensor site density and medium conditions), the FRET sensor (Fig. 1d) was also used to quantitatively detect PDGF. The non-specific background signal is minimized in this case because the signal produced is based on the ratio of decreased Cy3 fluorescence and increased Cy5 fluorescence (Supplementary Fig. S3). Moreover, the detection range of sensors on the cell surface spans from several hundred pM to low nM levels, which is within the range of serum PDGF concentrations (400–700 pM under physiological conditions, or higher under pathological conditions such as tumours)^{36,37}. Data from both the quench sensor and the FRET sensor in different culture media (PBS–/–, PBS +/+ and MSC medium with 15% fetal bovine serum (FBS)) are presented in Supplementary Fig. S4.

Spatial-temporal sensing using sensor-engineered cells

To determine whether sensors on cells produce a fluorescence signal in real time that can be resolved with high spatial resolution at the single-cell level, PDGF was added in close proximity to the cells through a micromanipulator-mounted microneedle coupled to a microinjector (Supplementary Fig. S5). Fluorescence imaging showed spatial variation of the signal intensity over the cell surface, which evolved over time as more PDGF was transported by the impinging flow to the cell surface (Fig. 4a). We also simulated the evolution of PDGF concentration in the vicinity of a cell using a three-dimensional unsteady convection–diffusion mass transport model (described in the Supplementary Information and Fig. S6). The evolution of PDGF concentrations on the surface of the cell was consistent with the observed fluorescence quenching behaviour; the model predicted a transition of the PDGF concentration in the vicinity of the cell from 0 nM at $t = 0$ to 40 nM at $t = 6$ s (Fig. 4b). Given that this aptamer sensor, when attached on the cell surface, detects PDGF in the range of ~1–10 nM (Fig. 3b), the timescale of a cell response is consistent with the timescale required for the PDGF concentration to change.

The development of sensors that can be used to examine cell-to-cell communication in real time at a single-cell level is invaluable for elucidating mechanisms of intercellular communication. Based on a microwell assay developed by Love and co-workers³⁸, we show that our sensor MSCs can detect PDGF secreted by neighbouring cells. On a polymeric substrate containing an array of microwells, we added sensor-modified MSCs and PDGF-producing MDA-MB-231 cells³⁹ (PDGF production was confirmed and quantified by ELISA; see Supplementary Methods). Cells settle by gravity into the microwells, which contain subnanolitre volumes (0.1 nl) with different combinations of cell ratios (sensor MSC:PDGF-producing MDA-MB-231 cells 1:0, 1:1, 1:2, 1:3+; Fig. 5). The fluorescence signal of the sensor MSCs was imaged continuously over time (6 h) as PDGF was produced by the MDA-MB-231 cell. As shown in Fig. 5, sensors on the MSC surface indeed produced a fluorescence signal that correlated directly with the number of MDA-MB-231 cells in the same microwell with the sensor MSC. In contrast, no significant signal difference was

observed in the sensor signal when sensor MSCs were incubated alone or with native MDA-MB-231 cells (not engineered to secrete PDGF; Supplementary Fig. S7).

***In vivo* monitoring of sensor-engineered cells**

As a first step towards using cell surface sensors to monitor the cellular environment, cell function and intercellular signalling *in vivo*, we tested the feasibility of using IVM to monitor the engineered cells after transplantation. To examine if aptamer conjugation affects the natural homing ability of MSC to bone marrow, both native and aptamer-MSC were injected simultaneously into Balb/c mice, and bone marrow imaging was performed 24 h post-injection⁴⁰. Using a fluorescence confocal and multiphoton intravital imaging system that tracks single cells in living animals, we observed ~30 cells per image stack for both sensor-engineered MSCs and native MSCs (Fig. 6a,b,c). The transendothelial migration of aptamer-MSC and unmodified MSC was not statistically different, $P = 0.116$ (Fig. 6d).

Given that the FRET system is desirable for *in vivo* studies as it provides a ratio of two distinct fluorescent dyes, thereby minimizing the non-specific background signal, we designed a simple oligonucleotide (FRET-probe, Supplementary Table S1) to address whether we could sense a change in FRET signal in a live mouse. The FRET probe carries Cy3 and Cy5 in close proximity, which initially projects a Cy5 signal when exciting Cy3. To examine if the FRET probe was viable in bone marrow *in vivo* (a key requirement for our sensor to work), we performed acceptor photo-bleaching of the Cy5 moiety *in situ* using a 635 nm laser, and a switch from Cy5 (red) to Cy3 (green) signal resulted (Supplementary Fig. S8). This experiment clearly suggests that it is feasible to use IVM to track transplanted sensor-engineered cells and monitor their signalling with the target molecules in their *in vivo* niche environment.

Conclusions

We have developed a simple cell-surface sensor platform that permits signalling to be monitored within the cellular environment, in real time, *in vitro* and potentially *in vivo*. Aptamer sensors can be readily modified with sensing molecules and surface anchors, and the binding affinity, folding and secondary structures can be engineered by mutating the aptamer sequences (Fig. 1)⁴¹. Furthermore, aptamer sensors for a large variety of target molecules can be obtained using (automated) SELEX^{14–20,42,43}. We have shown that MSCs engineered with an aptamer can be detected in mouse bone marrow by IVM 24 h post-transplantation, and the communication between FRET dyes is retained, suggesting that nucleic-acid-sensor conjugated fluorophores are functional on the cell surface for at least one day under physiological conditions. If required, nucleic acid stability towards nuclease degradation *in vivo* can be improved without impairing the binding affinity and signalling performance by incorporating protecting groups such as poly(ethylene glycol) (PEG), phosphorothioates and locked nucleic acids⁴¹.

We are currently engineering a reversible ‘structure switching’^{44,45} PDGF aptamer that has a covalent linker and complementary DNA (cDNA) that will compete with PDGF binding. Through this approach, when the PDGF concentration decreases, the bound PDGF, which is in competition with the cDNA, will dissociate quickly, allowing the rise and fall of signals to be monitored in real time.

Our cell surface sensors can be resolved spatiotemporally at the single-cell level (Fig. 4) and this is significant because cells respond to cues in their microenvironment in both time and space⁴⁶. Furthermore, the sensor could respond quantitatively to PDGF added to the culture medium or secreted by adjacent cells. This is useful for reporting on the state of cell signalling under physiological or pathological conditions such as inflammation. The 49 mer

PDGF sensor sequence used in this study is ~16 nm when fully stretched in a duplex format⁴⁷, and is expected to adopt a three-dimensional, tertiary structure upon binding to PDGF, leading to a dynamic radius less than ~8 nm. At this scale, the aptamer sensors sense signalling molecules at or near the cell surface. Note also that the local cytokine concentration in the vicinity of the cell surface is often distinct from the bulk medium because of delayed diffusion due to unstirred layer effects or degradation by cell-surface enzymes⁴⁸. Our approach may therefore provide significant advantages over traditional *in vitro* techniques (such as ELISA) that can only assess bulk concentration of cytokines, and may serve as a new tool to quantitatively measure signalling molecules or potentially drugs at the cell surface with high spatiotemporal resolution under physiological conditions.

Our long-term goal is to use the natural homing ability of specific cell types to deliver sensors to particular niches (such as bone marrow, lymph nodes, inflamed tissue or tumours) to monitor inter-cellular communication in real time *in vivo*. Cell homing is a specific and highly regulated, multistep process that includes cell rolling, adhesion and transendothelial migration and is mediated by specific receptor–ligand interactions². Direct placement of sensors into such environments would otherwise not be feasible without an invasive approach that may affect cell signalling. An important component of our approach is the use of IVM to monitor single cells in real time in living animals, and at a temporal and spatial resolution that is not presently possible with other techniques^{1,30–32}.

Previously, we and others have applied IVM to study the trafficking of leukocytes, haematopoietic stem cells and MSCs^{31,32} (D. Sarkar *et al.*, unpublished observations). In such studies, cells are typically labelled with lipophilic dyes or fluorescent proteins that can ‘passively’ indicate the location of a cell, but cannot report the phenotype or the properties that define the cellular microenvironment. In contrast, the cell-surface sensor approach makes use of functional aptamer sensors that dynamically monitor intercellular signalling in real time. Our ongoing work focuses on further engineering our FRET sensor to have a high signal-to-noise ratio under physiological conditions to monitor PDGF levels produced in the MSC niche by activated endothelial cells, tumour cells or in response to injury. In our experience, a signal-to-noise ratio of >4 is required for *in vivo* imaging. This work will ultimately lead to a better understanding of MSC biology, particularly in PDGF-signalling, including tissue regeneration, angiogenesis, immunomodulatory and tumour modelling^{24–26}.

Finally, chemistry-based cell engineering approaches have recently been developed to study cell-immobilized signalling moieties both *in vitro* and *in vivo* in living animals^{4,5,49}. For example, Bertozzi *et al.* reported the labelling of fluorophores on glycans using click chemistry in zebrafish, which permitted them to visualize glycan expression *in vivo*⁴. It is conceivable that in addition to labelling exogenous transplanted cells, the site-specific labelling of endogenous cells with ‘sensing molecules’ may become a valuable tool with which to monitor physiological and pathological changes *in vivo*. We anticipate that our study will serve as a gateway for the future development of a large toolkit of cell-surface sensors that biologists could routinely apply to elucidate cell biology both *in vitro* and *in vivo*.

Methods

Engineering aptamer sensors onto the MSC surface

MSCs (~1 M after trypsinization) (see Supplementary Information for routine MSC culture) were dispersed in biotin–NHS solution (1 mM in PBS–/–, 1 ml), and the solution was allowed to incubate for 10 min at room temperature. After washing, streptavidin solution (50 $\mu\text{g ml}^{-1}$ in PBS–/–, 1 ml) was then used to treat the cells for 5 min. Finally, biotin-modified sensor solution (two DNA strands were first annealed at 5 μM each in PBS +/+ at 90 °C for

3 min and cooled at room temperature for 30 min, 200 μ l) was added, and the suspension was incubated for 5 min at room temperature. The cells were then washed once by PBS $^{-/-}$ and subsequently used for experimentation. The fluorescent nature of the sensors allowed the conjugation step to be easily followed by flow cytometry (BD FACS Calibur flow cytometer) then analysed using Cell Quest software.

Microneedle experiment

Microneedle experiments were performed using a microinjector (FemtoJet, Eppendorf) with Eppendorf Femtotips and an Eppendorf micromanipulator (InjectMan NI 2, Eppendorf) (Supplementary Fig. S5). Glass microneedles with inner tip diameters of \sim 3 μ m were made using a micropipette puller (P-97 Sutter Instrument Company). Microneedles were backfilled with the PDGF (2 μ M in PBS $^{-/-}$) using Eppendorf Femtotips Capillary Pipet Tips Microloaders. The microneedle, controlled by a micromanipulator, was lowered onto a dish with sensor-engineered MSCs settled on the surface in PBS $^{-/-}$, positioned at a defined lateral distance (\sim 40 μ m) from the settled cells and at a height of \sim 30 μ m from the underlying substrate. PDGF was released from the micropipette by applying a defined pressure (26 hPa). Simultaneously, phase contrast and fluorescence images of the cells were collected sequentially with a 1 s interval exposure time. Between 10 and 12 cells were measured in each experiment.

Computational model for PDGF transport in microneedle experiment

See Supplementary Information.

Cell-cell communication microwell assay and analysis

Time-course microwell assays were performed following previously reported protocols with some modifications³⁸. The fabrication of the microwell is presented in the Supplementary Information. A sensor MSC suspension (1×10^5 cells/ml) was first placed on the surface of the array and cells were permitted to settle into the microwells by gravity. After 2 min, excess cells were washed away with serum-free media. Next, PDGF-producing MDA-MB-231 cells (1×10^5 cells/ml) in medium containing 15% FBS were loaded into the wells as described above. After a brief incubation at 37 $^{\circ}$ C with 5% CO₂, the array was delivered to the microscope for imaging. All images were acquired on an automated inverted fluorescence microscope (Zeiss Observer Z-1, Carl Zeiss Inc.) equipped with a stage incubator (PM S1) and incubation chamber for live-cell imaging (37 $^{\circ}$ C, 5% CO₂). Phase and fluorescence (GFP and Cy5) micrographs were collected every 3 min for 6 h. A total of 3000 microwells were imaged at each time point. A custom-written image analysis program was used to identify the location and fluorescence intensity of each cell in the microwell array, as described previously³⁸. A MATLAB script was written to track the fluorescence signal intensity of each sensor MSC over the 6 h time course. The signal intensity of each sensor MSC was normalized to the signal intensity at $t = 0$ min to account for the baseline cell-to-cell variation in sensor MSC intensity. Sensor MSCs were divided into groups based on the number of PDGF-producing MDA-MB-231 cells residing in the same microwell (0, 1, 2 or 3+). More than 100 MSCs (see Fig. 5 for exact numbers) from each group were tracked. The fraction of sensor MSCs in each group with signal intensity less than 50% of the initial signal intensity was calculated at each time point.

Supplementary Material

Refer to Web version on PubMed Central for supplementary material.

Acknowledgments

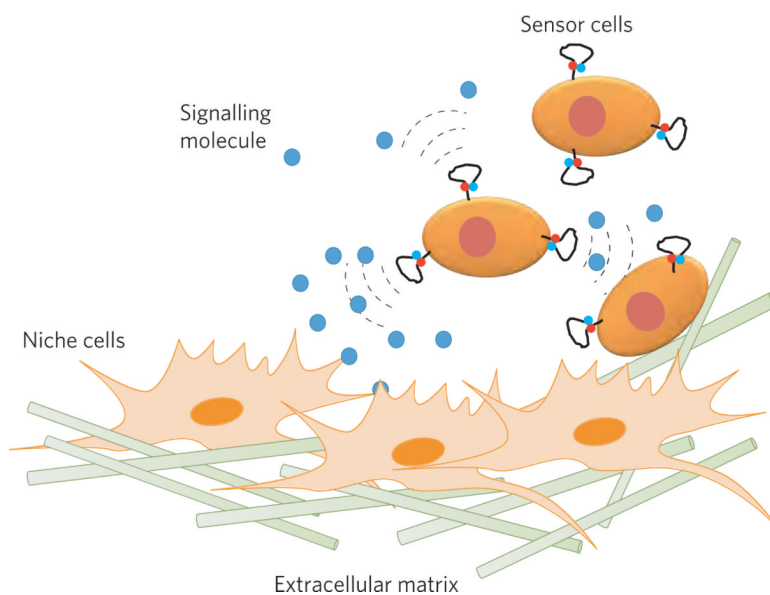
The authors thank Lei Xu and Dannie Wang for the preparation of PDGF-producing MDA-MB-231 cells. This work was supported by the National Institutes of Health (NIH; grants nos. HL097172, HL095722 and DE019191 to J.M.K., grants nos. HL082792 and NS059348 to J.L., and grant no. NIAID 5RC1AI086152 to J.C.L.), by the Charles A. Dana Foundation (J.C.L.) and by the American Heart Association (grant no. 0970178N to J.M.K.). W.Z. is supported by an International Human Frontier Science Program Organization postdoctoral fellowship. Y.J.Y. holds a National Science Foundation Graduate Fellowship.

References

- Halin C, Mora J, Sumen C, von Andrian U. *In vivo* imaging of lymphocyte trafficking. *Annu. Rev. Cell. Dev. Biol.* 2005; 21:581–603. [PubMed: 16212508]
- Karp JM, Teo G. Mesenchymal stem cell homing: the devil is in the details. *Cell Stem Cell.* 2009; 4:206–216. [PubMed: 19265660]
- Ferreira L, Karp JM, Nobre L, Langer R. New opportunities: the use of nanotechnologies to manipulate and track stem cells. *Cell Stem Cell.* 2008; 3:136–146. [PubMed: 18682237]
- Laughlin ST, Baskin JM, Amacher SL, Bertozzi CR. *In vivo* imaging of membrane-associated glycans in developing zebrafish. *Science.* 2008; 320:664–667. [PubMed: 18451302]
- Cook BN, Bertozzi CR. Chemical approaches to the investigation of cellular systems. *Bioorg. Med. Chem.* 2002; 10:829–840. [PubMed: 11836089]
- Giepmans BNG, Adams SR, Ellisman MH, Tsien RY. The fluorescent toolbox for assessing protein location and function. *Science.* 2006; 312:217–224. [PubMed: 16614209]
- Hoffmann C, et al. A FIAsh-based FRET approach to determine G protein-coupled receptor activation in living cells. *Nature Methods.* 2005; 2:171–176. [PubMed: 15782185]
- Pollok BA, Heim R. Using GFP in FRET-based applications. *Trends Cell Biol.* 1999; 9:57–60. [PubMed: 10087619]
- Modi S, et al. A DNA nanomachine that maps spatial and temporal pH changes inside living cells. *Nature Nanotech.* 2009; 4:325–330.
- Albizu L, et al. Time-resolved FRET between GPCR ligands reveals oligomers in native tissues. *Nature Chem. Biol.* 2010; 6:587–594. [PubMed: 20622858]
- Rider T, et al. A B cell-based sensor for rapid identification of pathogens. *Science.* 2003; 301:213–215. [PubMed: 12855808]
- Beigi R, Kobatake E, Aizawa M, Dubyak G. Detection of local ATP release from activated platelets using cell surface-attached firefly luciferase. *Am. J. Physiol. Cell Physiol.* 1999; 276:C267–C278.
- Orynbayeva Z, et al. Visualization of membrane processes in living cells by surface-attached chromatic polymer patches. *Angew. Chem. Int. Ed.* 2005; 44:1092–1096.
- Tuerk C, Gold L. Systematic evolution of ligands by exponential enrichment: RNA ligands to bacteriophage T4 DNA polymerase. *Science.* 1990; 249:505–510. [PubMed: 2200121]
- Ellington A, Szostak J. *In vitro* selection of RNA molecules that bind specific ligands. *Nature.* 1990; 346:818–822. [PubMed: 1697402]
- Liu J, Cao Z, Lu Y. Functional nucleic acid sensors. *Chem. Rev.* 2009; 109:1948–1998. [PubMed: 19301873]
- Zhao W, Brook M, Li Y. Design of gold nanoparticle based colorimetric biosensing assays. *ChemBioChem.* 2008; 9:2363–2371. [PubMed: 18821551]
- Sefah K, et al. Nucleic acid aptamers for biosensors and bio-analytical applications. *Analyst.* 2009; 134:1765–1775. [PubMed: 19684896]
- Nutiu R, Li Y. *In vitro* selection of structure-switching signaling aptamers. *Angew. Chem. Int. Ed.* 2005; 44:1061–1065.
- Keefe AD, Pai S, Ellington A. Aptamers as therapeutics. *Nature Rev. Drug Discov.* 2010; 9:573–550.
- Fang X, Tan W. Aptamers generated from cell-SELEX for molecular medicine: a chemical biology approach. *Acc. Chem. Res.* 43:48–57. [PubMed: 19751057]

22. Dhar S, Kolishetti N, Lippard SJ, Farokhzad OC. Targeted delivery of a cisplatin prodrug for safer and more effective prostate cancer therapy *in vivo*. *Proc. Natl Acad. Sci. USA*. 108:1850–1855.
23. Ankrum J, Karp JM. Mesenchymal stem cell therapy: two steps forward, one step back. *Trends Mol. Med.* 2010; 16:203–209. [PubMed: 20335067]
24. López Ponte A, et al. The *in vitro* migration capacity of human bone marrow mesenchymal stem cells: comparison of chemokine and growth factor chemotactic activities. *Stem Cells*. 2007; 25:1737–1745. [PubMed: 17395768]
25. Beckermann B, et al. VEGF expression by mesenchymal stem cells contributes to angiogenesis in pancreatic carcinoma. *Br. J. Cancer*. 2008; 99:622–631. [PubMed: 18665180]
26. Ball SG, Shuttleworth CA, Kielty CM. Mesenchymal stem cells and neovascularization: role of platelet-derived growth factor receptors. *J. Cell. Mol. Med.* 2007; 11:1012–1030. [PubMed: 17979880]
27. Fang X, Sen A, Vicens M, Tan W. Synthetic DNA aptamers to detect protein molecular variants in a high-throughput fluorescence quenching assay. *ChemBioChem*. 2003; 4:829–834. [PubMed: 12964156]
28. Vicens M, Sen A, Vanderlaan A, Drake T, Tan W. Investigation of molecular beacon aptamer-based bioassay for platelet-derived growth factor detection. *ChemBioChem*. 2005; 6:900–907. [PubMed: 15812865]
29. Green LS, et al. Inhibitory DNA ligands to platelet-derived growth factor B-chain. *Biochemistry*. 1996; 35:14413–14424. [PubMed: 8916928]
30. Adams GB, et al. Haematopoietic stem cells depend on Gα(s)-mediated signalling to engraft bone marrow. *Nature*. 2009; 459:103–107. [PubMed: 19322176]
31. Lo Celso C, et al. Live-animal tracking of individual haematopoietic stem/progenitor cells in their niche. *Nature*. 2009; 457:92–97. [PubMed: 19052546]
32. Lo Celso C, Wu JW, Lin CP. *In vivo* imaging of hematopoietic stem cells and their microenvironment. *J. Biophoton*. 2009; 2:619–631.
33. Sarkar D, et al. Chemical engineering of mesenchymal stem cells to induce a cell rolling response. *Bioconjug. Chem*. 2008; 19:2105–2109. [PubMed: 18973352]
34. Sarkar D, et al. Engineered mesenchymal stem cells with self-assembled vesicles for systemic cell targeting. *Biomaterials*. 2010; 31:5266–5274. [PubMed: 20381141]
35. Zhao W, et al. Mimicking the inflammatory cell adhesion cascade by nucleic acid aptamer programmed cell–cell interactions. *FASEB J*. 2011 doi:10.1096/fj.10-178384.
36. Lai RY, Plaxco KW, Heeger AJ. Aptamer-based electrochemical detection of picomolar platelet-derived growth factor directly in blood serum. *Anal. Chem*. 2007; 79:229–233. [PubMed: 17194144]
37. Leitzel K, et al. Elevated plasma platelet-derived growth factor B-chain levels in cancer patients. *Cancer. Res*. 1991; 51:4149–4154. [PubMed: 1868437]
38. Ogunniyi AO, Story CM, Papa E, Guillen E, Love JC. Screening individual hybridomas by microengraving to discover monoclonal antibodies. *Nature Protoc*. 2009; 4:767–782. [PubMed: 19528952]
39. Au P, et al. Paradoxical effects of PDGF-BB overexpression in endothelial cells on engineered blood vessels *in vivo*. *Am. J. Pathol*. 2009; 175:294–302. [PubMed: 19477947]
40. Mazo IB, et al. Hematopoietic progenitor cell rolling in bone marrow microvessels: parallel contributions by endothelial selectins and vascular cell adhesion molecule 1. *J. Exp. Med*. 1998; 188:465–474. [PubMed: 9687524]
41. Jayasena S. Aptamers: an emerging class of molecules that rival antibodies in diagnostics. *Clin. Chem*. 1999; 45:1628–1650. [PubMed: 10471678]
42. Cox JC, Rudolph P, Ellington AD. Automated RNA selection. *Biotechnol. Prog*. 1998; 14:845–850. [PubMed: 9841645]
43. Lou X, et al. Micromagnetic selection of aptamers in microfluidic channels. *Proc. Natl Acad. Sci. USA*. 2009; 106:2989–2994. [PubMed: 19202068]

44. Kim G, Kim K, Oh M, Sung Y. The detection of platelet derived growth factor using decoupling of quencher-oligonucleotide from aptamer/quantum dot bioconjugates. *Nanotechnology*. 2009; 20:175503. [PubMed: 19420593]
45. Tang Z, et al. Aptamer switch probe based on intramolecular displacement. *J. Am. Chem. Soc.* 2008; 130:11268–11269. [PubMed: 18680291]
46. Hui E, Bhatia S. Micromechanical control of cell–cell interactions. *Proc. Natl Acad. Sci. USA*. 2007; 104:5722–5726. [PubMed: 17389399]
47. Zhao W, Gao Y, Kandadai SA, Brook MA, Li Y. DNA polymerization on gold nanoparticles through rolling circle amplification: towards novel scaffolds for three-dimensional periodic nanoassemblies. *Angew. Chem. Int. Ed.* 2006; 45:2409–2413.
48. Hayashi S, Hazama A, Dutta AK, Sabirov RZ, Okada Y. Detecting ATP release by a biosensor method. *Sci. STKE*. 2004; 2004:pl14. [PubMed: 15536175]
49. Zhao W, Teo G, Kumar N, Karp J. Chemistry and material science at the cell surface. *Mater. Today*. 2010; 13:14–21.

**Scheme 1.**

Probing the cellular niche environment and signalling using cells engineered with an aptamer sensor. Aptamer sensors that bind to signalling molecules (PDGF in this case) are covalently attached to the surface of cells (mesenchymal stem cells in this case). Signalling molecules secreted by niche cells are detected by the sensor cells, and the fluorescent signal generated is measured.

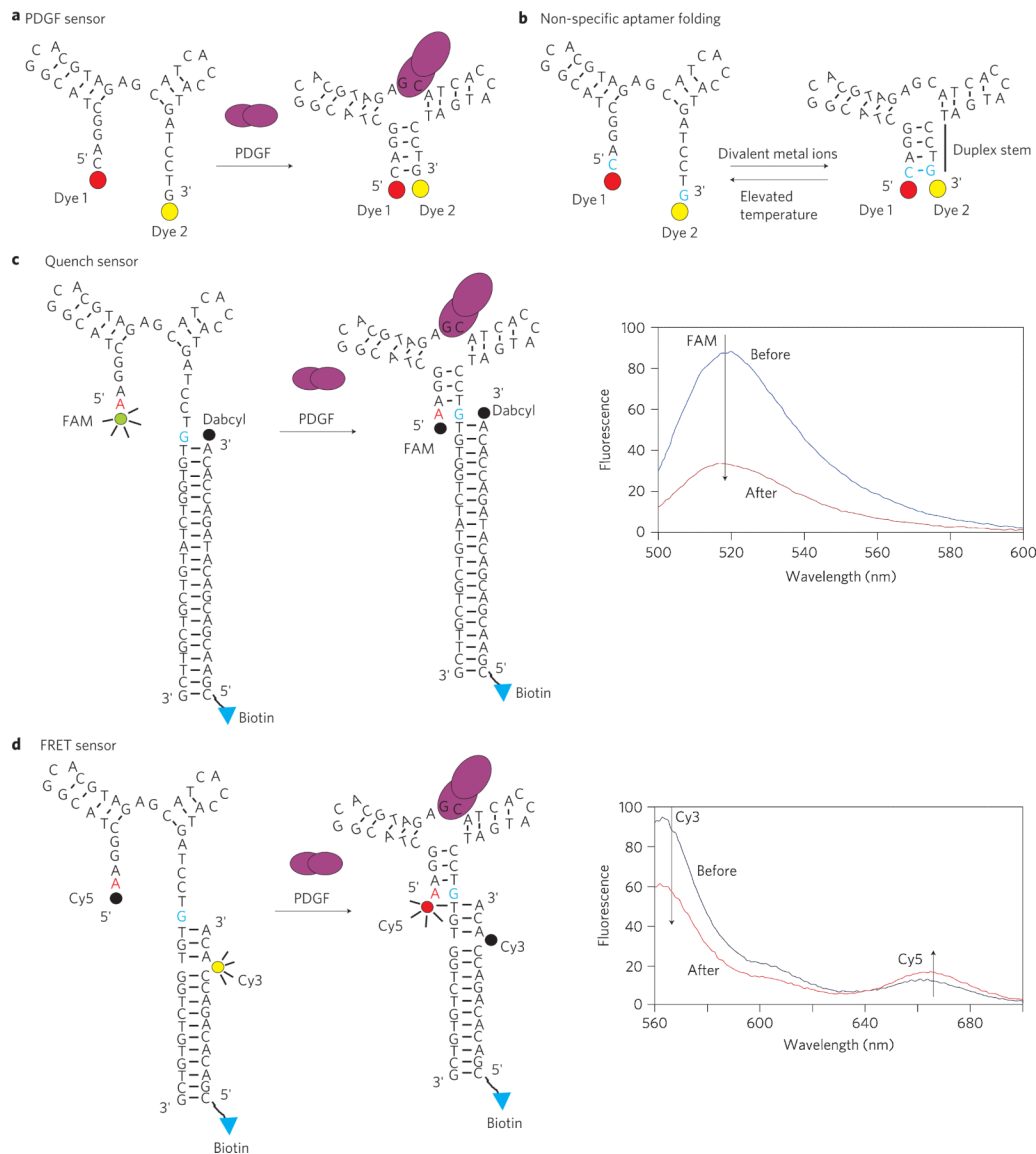


Figure 1. Mechanism of PDGF aptamer sensors in solution

a, Original PDGF sensor described in ref. 28. When bound to PDGF, the aptamer changes from an open structure to a complex with paired bases in the stem region. The two dyes are located closer to one another and yield a fluorescent signal. **b**, Non-specific folding of the original sensor at elevated ionic strength in the presence of divalent metal ions. **c,d**, Engineered sensors. The terminal C–G base pair (blue) is mutated to an A–G pair (red–blue) for less non-specific folding in the aptamer. Biotin moieties allow immobilization on the cell surface. In the quench sensor (**c**), fluorescence of the FAM dye is quenched by a quencher molecule (Dabcyl) in the presence of 10 nM PDGF in PBS^{-/-}. In the FRET sensor (**d**), donor dye (Cy3) fluorescence decreases and acceptor dye (Cy5) fluorescence increases upon addition of 10 nM PDGF in PBS. Spectra in **c** and **d** were recorded at room temperature.

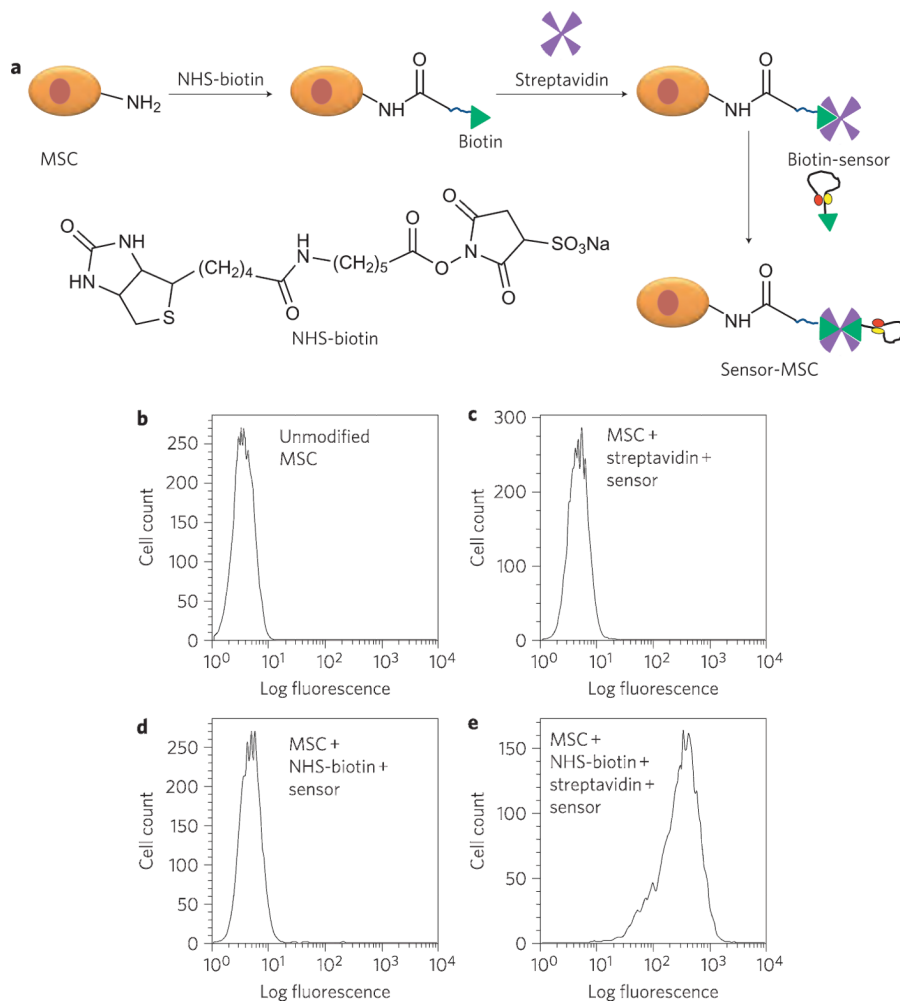


Figure 2. Anchoring the engineered aptamer sensor to the cell surface
a, Schematic showing the chemistry approach used to attach sensors to MSCs. **b–e**, Flow cytometry data using the Cy3 signal of the FRET sensor show successful conjugation of the aptamer sensor on the cell surface.

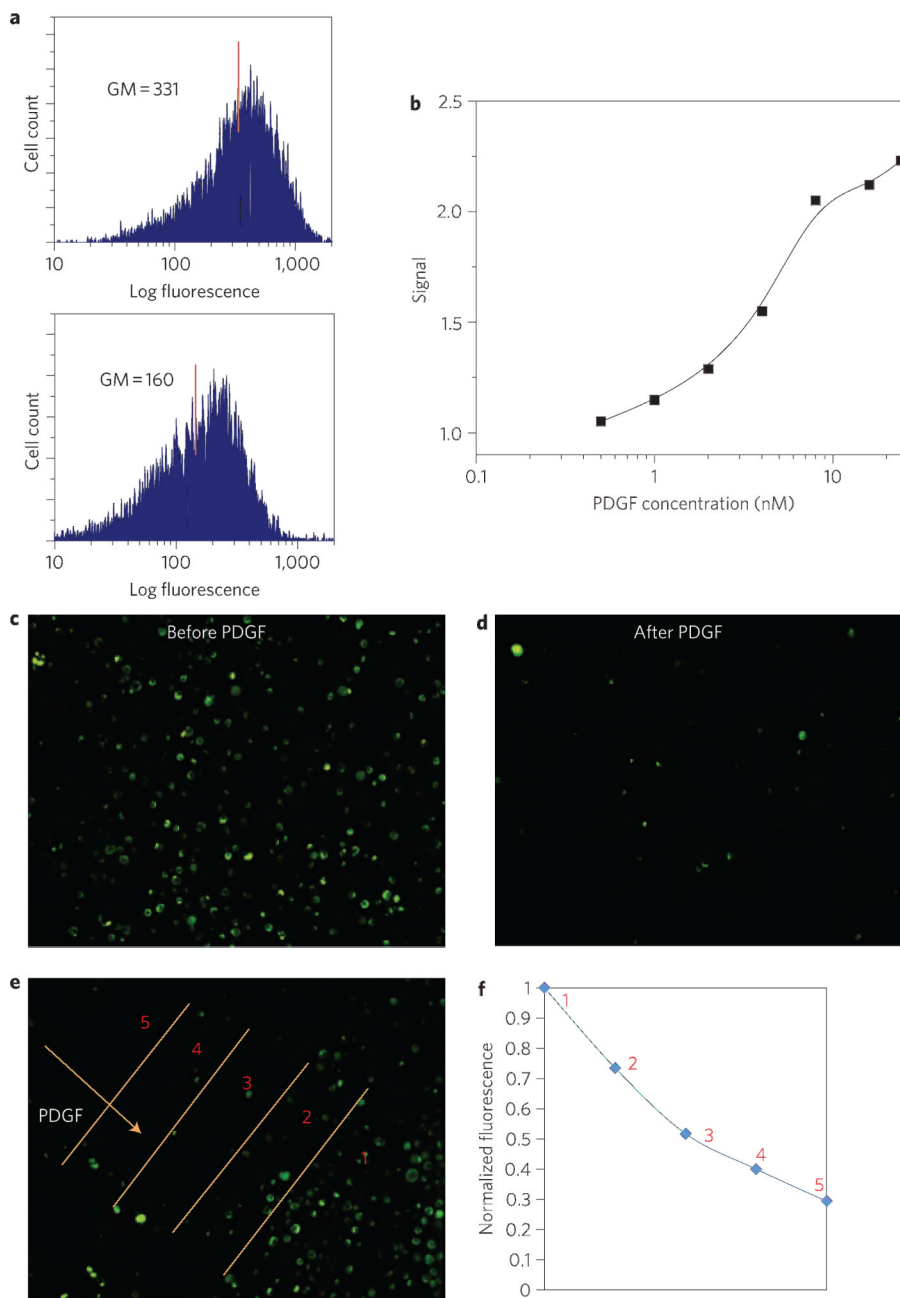


Figure 3. Aptamer sensor functions on the cell surface

a, Representative sensor performance data, examined using flow cytometry, for the quench sensor immobilized on the MSC surface before and immediately after addition of 10 nM PDGF (GM, geometric mean). **b**, Sensor signal (defined as the ratio of GM before and after addition of PDGF) versus concentration of PDGF in PBS^{-/-}. **c,d**, Representative fluorescent microscopy images of sensor cell before and immediately after addition of 10 nM PDGF in PBS^{-/-}, respectively. **e**, PDGF (2 μ M) was added to sensor-modified MSCs from the top/left corner (arrow shows direction) using a pipette tip, and the image was recorded immediately. **f**, The PDGF gradient was separated into five regions using image analysis, and the fluorescent intensities of 10 representative cells from each region were averaged and

plotted. The sensor signal in region 1 is defined as 1; other regions are normalized accordingly.

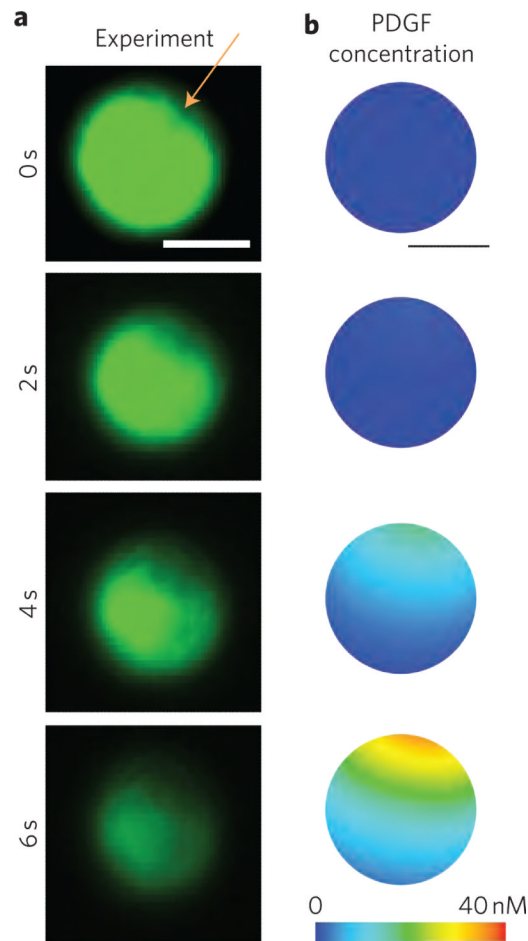


Figure 4. Spatial-temporal imaging of a single MSC functionalized with the quench sensor demonstrates that PDGF sensing correlates with data generated from a computational model
a, PDGF ($2\ \mu\text{M}$) was injected $30\ \mu\text{m}$ from the cell using a microneedle, as indicated by the orange arrow (Supplementary Fig. S5 includes a representative light microscope image showing the microneedle juxtaposed to the cell surface). The signal was quenched as PDGF engaged the sensor while moving across the cell surface as a function of time, as observed by fluorescent microscopy. **b**, Concentration of PDGF on the cell surface as predicted from a three-dimensional computational mass transport model (described in Supplementary Information). Scale bar, $10\ \mu\text{m}$.

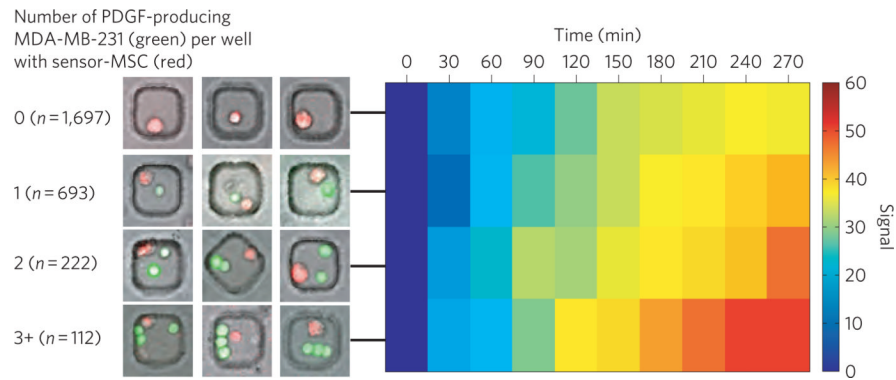


Figure 5. Real-time sensing of PDGF secretion from neighbouring MDA-MB-231 cells by sensor-engineered MSCs

Left panel: representative images of microwells containing different numbers of PDGF-producing MDA-MB-231 cells (green) in the same well with sensor MSC (red) at time $t = 0$ (n is the number of MSCs used in the analysis). MDA-MB-231 is genetically engineered to secrete PDGF that is fused with a GFP tag. To be distinguishable, the quench sensor in this set of experiments is labelled with a red dye (Cy5), and with Iowa Black RQ as a quencher. Cy5/Iowa Black RQ and FAM/Dabcyl perform similarly (Supplementary Fig. S9). Right panel: fluorescence of sensor MSC declining during the course of PDGF production. The signal, which is defined as the percentage of MSCs that have fluorescence intensity less than 50% of their initial value at the indicated time, correlates with the number of PDGF-producing MDA-MB-231 cells in the same well as a sensor MSC.

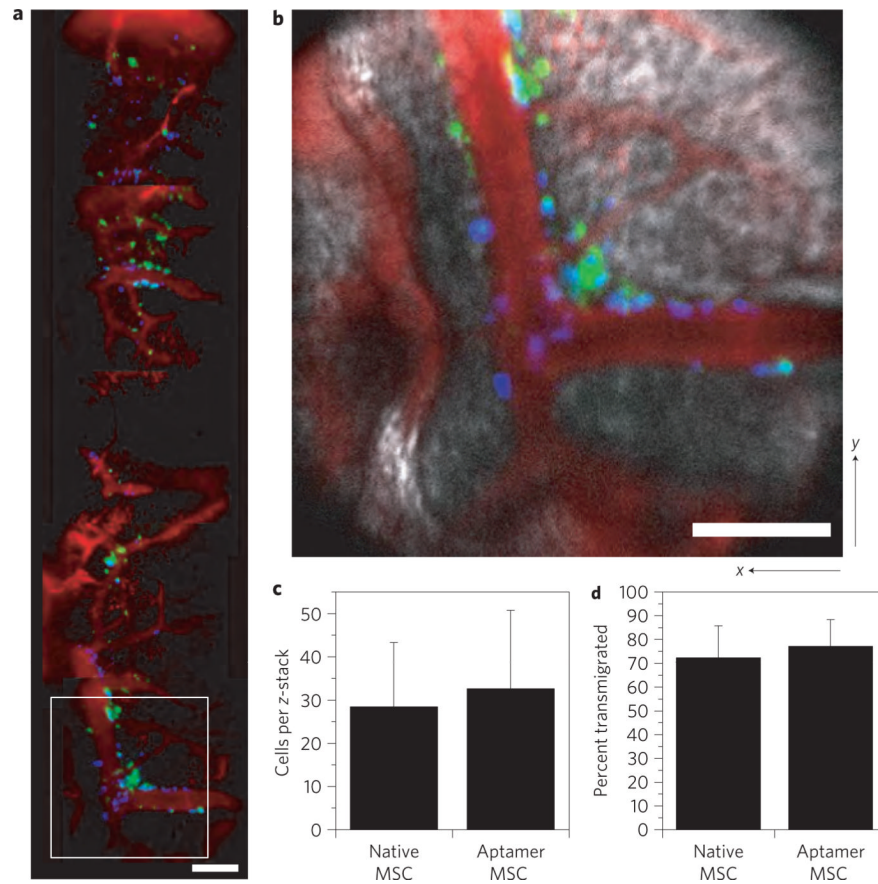


Figure 6. Bone marrow homing and transmigration of aptamer-labelled MSCs

a, Large-area map of right parietal bone marrow compartments in an eight-week-old Balb/c mouse 24 h after injection of MSC and aptamer-MSC. Several image stacks were acquired in the right parietal bone ~200 μm to the right of the sagittal suture. **b**, Zoomed-in image of the area in the white box in **a**, shows a similar distribution of MSC (green) and aptamer-MSC (blue) in the vicinity of a large venule (red). **c**, Quantification of the average number of cells per z-stack. **d**, Quantification of percentage of cells positioned outside blood vessels shows no difference between MSC and aptamer-MSC (P -value = 0.116). MSC, green; aptamer-MSC, blue; blood vessels, red; bone, white. Scale bar, 100 μm .